Version of Record: https://www.sciencedirect.com/science/article/pii/S1361920920308129
Manuscript_b76046a69029f0fc740f4b89c707f5c5

Multivariate and location-specific correlates of fuel consumption: A test track study

Timo Melman*+^, David Abbink+, Xavier Mouton*, Adriana Tapus^, Joost de Winter+
**Group Renault, Chassis Systems Department, 1 Avenue du Golf, 78280 Guyancourt, France*
+Department of Cognitive Robotics, Faculty 3mE, Delft University of Technology, Mekelweg 2, 2628 CD Delft, The Netherlands
^Department of Computer and System Engineering, ENSTA Paris, 828 Boulevard des Marchaux, 91762 Palaiseau Cedex, France
timo.melman@renault.com, T.Melman@tudelft.nl

Abstract

Current predictors of fuel consumption are typically based on computer simulations or data collections in real traffic, where the route and vehicle type are not under the researcher's control. Here, we predicted fuel consumption using test track data, an approach that allowed for location-specific predictions. Ninety-one drivers drove a total of 4617 laps, in two vehicles (Renault Mégane, Renault Clio), on two routes (highway and mountain), and with two eco-driving instructions (normal and eco). A multivariate analysis at the level of laps showed a strong predictive value for metrics related to speed, RPM, and throttle position, but with a considerable amount of variance attributable to route and vehicle type. A subsequent location-specific analysis showed that the predictive correlation of driving speed and throttle position fluctuated strongly during the lap and at some locations even became negative. We conclude that there is considerable potential in instantaneous location-specific prediction of fuel consumption.

Keywords: Eco-driving; Driving metrics; CAN-bus data; Principal component analysis (PCA); Test track

Highlights

- Measurements of eco-driving and normal-driving behaviour and fuel consumption were collected on a test track
- Driving metrics were found to have a strong predictive value for fuel consumption.
- A considerable amount of variance within the driving metrics was attributable to route type.
- A driver's total fuel consumption can be predicted instantaneously from location-specific behaviour.

© 2020 published by Elsevier. This manuscript is made available under the CC BY NC user license
https://creativecommons.org/licenses/by-nc/4.0/

1. Introduction

With the rise in CO2 levels in the atmosphere, the reduction of fuel consumption is becoming an increasingly important topic. Under the pressure of strict regulations, car manufacturers are forced to produce increasingly efficient vehicles. Not only the vehicle technology itself but also the behaviour of the driver has a significant impact on fuel consumption. Studies show that eco-driving can reduce fuel consumption, and thereby pollutant emissions (Ho et al., 2015; Saboohi & Farzaneh, 2009), by 5% if compared to normal driving, or even more if compared to aggressive driving (for reviews about the effect of eco-driving on fuel efficiency, see Alam & McNabola, 2014; Huang et al., 2018; Xu et al., 2016).

Various authors have investigated optimal fuel-efficient driving through computer simulations. Maintaining a constant speed, shifting up early, and avoiding excessive pedal movements have been shown to be essential factors in minimising fuel consumption (Dib et al., 2014; Saboohi & Farzaneh, 2009; Sarkan et al., 2019; Mensing et al., 2013). Mensing et al. (2013) concluded through computer simulations that, for optimal eco-driving, drivers should accelerate quickly to a relatively low cruising speed. They also recommended early and gentle deceleration, followed by late and hard braking. Whether these optimal behaviours are realistic or desirable was not discussed in their research. For example, while extreme late braking can be optimal in terms of fuel consumption, it is not something drivers would normally do for safety and comfort reasons.

Although it is known how drivers should behave to drive ecologically, relatively little information is available about how ecologically-friendly drivers actually drive. Knowing how drivers drive is important for developing eco-driving feedback and training (Allison & Stanton, 2018; Caban et al., 2019; Sanguinetti et al., 2020). For example, drivers could receive an eco-score on their dashboard that reflects the impact of their current driving behaviour on fuel consumption (Sanguinetti et al., 2020; Vaezipour et al., 2015). Such an eco-score should be calibrated on realistic human driving behaviour, not based on modelled behaviour that may not be acceptable in the real world.

Real-world studies provide relevant insight into individual differences in ecological driving styles (Ericsson, 2001; Lois et al., 2019). Ericsson (2001), for example, investigated driving behaviour data for 19,230 driving periods collected in real traffic. A significant variation in fuel consumption was observed, with an average of 10 litres per km and a standard deviation of about 6 litres per km. Among other things, it was found that engine

speeds above 3500 rpm explained part of the variance in fuel consumption. However, the strongest effect on fuel consumption was found for a "stop factor", which was related to the number of stops per kilometre and the percentage of time the vehicle was stationary. This finding is not necessarily due to individual differences in driving behaviour, but rather due to traffic conditions such as the presence of traffic lights along the route. What this finding shows is that naturalistic driving studies inherently contain confounding factors that hamper understanding of what constitutes fuel-efficient driving behaviour. In particular, such studies do not control external factors that influence fuel consumption, such as the presence of curves, inclinations, traffic lights, and the impact of surrounding traffic.

As noted above, there is a paucity of research on how drivers drive ecologically. Although route selection and trip planning have been cited as an important factor in reducing fuel consumption (Sanguinetti et al., 2017; Sivak and Schoettle, 2012; Zhou et al., 2016), field studies typically do not control for it. This problem was also recognised by Lois et al. (2019), who stated: "to the best of our knowledge, there are no studies in the literature that analyse key factors for fuel consumption and eco-driving, controlling external factors." In a field study, they measured the fuel consumption of 1156 trips from 24 drivers, and observed that external factors had a key role in fuel consumption. The authors created a statistical model in the form of a path analysis, which included two external factors that were found to be predictive of fuel consumption: road congestion and the slope of the road. Lois et al.'s method is a promising approach to controlling for route-related effects. Still, this method is not entirely satisfactory for understanding the effects of external factors, because the control for external factors was applied in the form of a statistical correction rather than an experimental manipulation.

In our work, we have attempted to close this research gap by using instrumented vehicles on a test track. The availability of a test track makes it possible to expose drivers to a specific route, measure fuel consumption on a meter-to-meter basis, and remove the influence of uncontrolled traffic elements such as traffic lights and other road users. The instrumented vehicles recorded the vehicle location using GPS along with CAN bus data. Drivers were given the task of either complying with an eco-score or driving as they normally would, for two instrumented vehicle types and two route types with fundamentally different characteristics. The first route type was a sharply curved mountain route and the second route type was a highway.

The purpose of this paper is to predict fuel consumption from driving behaviour measurements, in order to allow informed design choices for eco-driving feedback and training applications. We use two methods of predicting fuel consumption: a multivariate analysis at the level of a trip (defined herein as a lap on the mountain or highway route in a given vehicle) and a location-specific method. We show, using the first method, that driving metrics have a strong predictive value for fuel consumption, and that a large part of the variance in the driving metrics is attributable to the route type and the vehicle type. These sources of variance would be a disturbance when predicting fuel consumption from driving metrics based on different routes and vehicles combined. Another limitation of trip-related metrics is that valuable information is lost due to the aggregation of, for example, driving behaviour on curves and straights. In the second part of this paper, we demonstrate that it is sensible to develop location-specific predictors of eco-driving. In this study, a location-specific predictor refers to driving behaviours (e.g., throttle position) at a specific travelled distance along the lap on the test track. More specifically, we correlated drivers' behaviours on a meter-to-meter basis with their fuel consumption for all other laps driven (leave-one-out validation). By means of a location-specific analysis, route features that can impact fuel consumption, such as curvature and road inclination, are implicitly controlled. Finally, we make conclusions and recommendations for location-specific fuel consumption predictions.

2. Method

This study uses data initially collected to monitor the wear of vehicle components. In this study, we use this data for the above-described purpose.

2.1 Participants

Ninety-one test drivers from Renault participated in this study. All participants regularly drove on the test track and were familiar with both routes (highway and mountain) and vehicle types (Renault Mégane and Renault Clio). These drivers were not professional test drivers; that is, their primary job did not consist of testing vehicle performance. Due to Renault's ethical and privacy protocols, driver-related information regarding age, gender, and yearly mileage cannot be made public.

2.2. Vehicles

Two vehicle types were used in this experiment: a Renault Mégane IV and Renault Clio IV (Table 1), both having a manual transmission.

Table 1. Vehicle information for the two types of vehicles used in this experiment.

Vehicle type	**Year of manufacture**	**Engine model**	**Fuel type**	**Engine displacement (cm^3)**	**Max Power (hp)**	**Curb weight (kg)**	**Emission legislation**	**Wheelbase length (mm)**
Renault Clio	2017	K9K 628	Diesel	1461	90	1071	Euro 5	2589
Renault Mégane	2017	K9K 656	Diesel	1461	110	1205	Euro 6	2669

For each vehicle type, two identical vehicles were used for the experiment: one for eco-driving and one for normal driving, resulting in a total of four vehicles used in this experiment. These four vehicles were equipped with a GPS tracker and a CAN-bus that allowed for recording signals associated with vehicle motion, steering, and pedal movements at a sampling frequency of 100 Hz.

2.3. Route types

This experiment was performed on Renault's test circuit in Aubevoye, France. Two types of routes were used in this study: a 4.1 km long highway section containing a two-lane highway with a recommended speed of 100 km/hr, and a 5.7 km long two-lane mountain section with a maximum altitude difference of approximately 50 m. The highway sections and mountain sections were extracted from the total dataset using the recorded GPS locations, as shown in Figure 1. The routes did not feature intersections or traffic lights. Table 2 shows the total number of laps driven per task instruction, route type, and vehicle type. Appendix A provides an overview of the driven conditions for all 91 participants.

Table 2. The number of participants who drove with and without eco-score feedback, for the highway and mountain, and for the Mégane and the Clio.

	Normal				**Eco-driving**			
	Highway		**Mountain**		**Highway**		**Mountain**	
	Mégane	**Clio**	**Mégane**	**Clio**	**Mégane**	**Clio**	**Mégane**	**Clio**
Number of drivers	34	25	24	21	35	34	23	26
Total laps driven	665	585	449	481	784	665	536	452

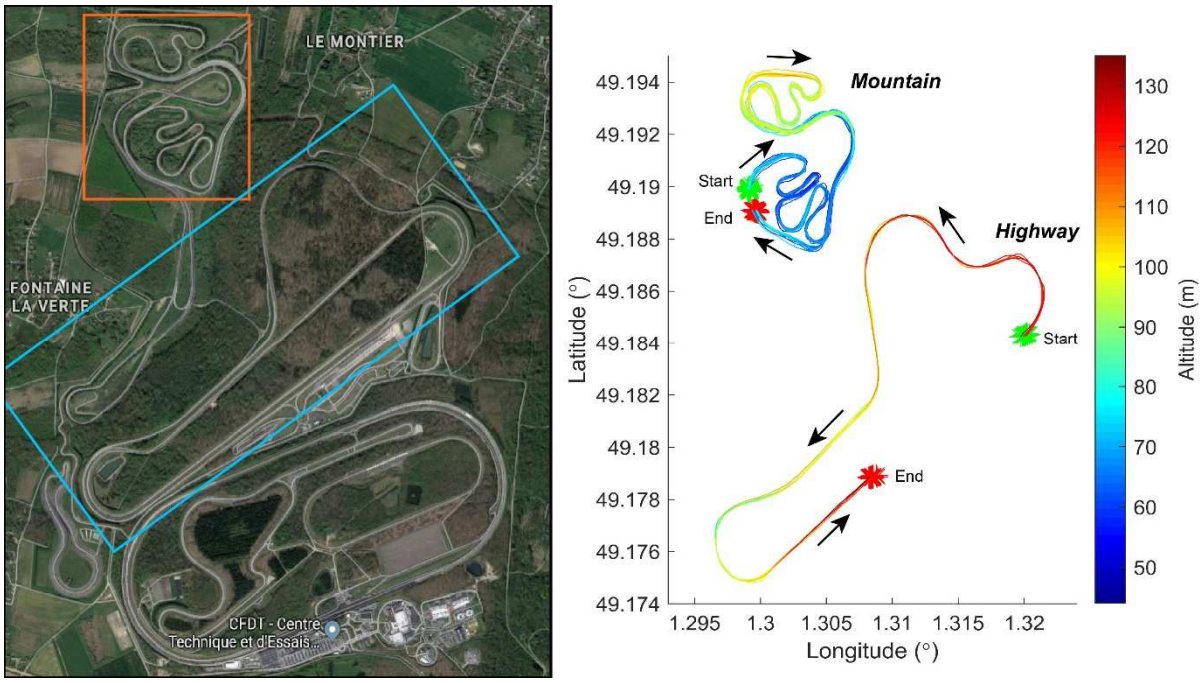


Figure 1. Left: top view of the route types (mountain and highway). Right: an example of the GPS data for the route types. The start and end-points are visualised with a green and red asterisk, respectively. The driving direction is indicated by arrows.

2.4. Eco-driving training

In this experiment, two task instructions were given: an eco-instruction to drive as economically as possible, and a normal driving instruction. If drivers were assigned to the 'normal' task, they were asked to drive as they normally would. If drivers were assigned to the eco-driving task, they were asked to drive with an average Renault eco-score of at least 90% of 100%. The eco-score, ranging from 0% (non-eco) to 100% (eco), is a Renault in-house developed score, computed from longitudinal accelerations/decelerations, driving speed, and late gear changing behaviour (i.e., driving with a high engine RPM). A Renault expert trained five group leaders, who, in turn, trained the rest of the participants identically. During the two-hour training, the participants first drove on the test track with their own driving style. After this run, the eco-expert gave advice on speed, acceleration, braking, and shifting behaviour to optimise fuel consumption.

2.5. Experimental protocol

The data were collected 24 hours a day over a period of 3.5 months. Every 8 hours, two drivers were assigned a vehicle and had to drive approximately 300 km. No specific instructions were given on where to drive. Drivers

did not know that the highway and mountain sections were extracted and analysed separately. While driving, the average eco-score of the session was shown as a number on the display.

2.6. Part 1: Predicting fuel consumption from lap-level metrics

2.6.1. Measured CAN-bus signals

From the CAN-bus data, 11 signals were obtained/derived. These signals reflect longitudinal driving behaviour (7 signals), lateral driving behaviour (3 signals), as well as fuel consumption (see Table 3, left column for the 10 longitudinal and lateral signals). The speed x longitudinal acceleration signal (va) is known to be predictive of fuel consumption (Ericsson, 2001) and is a surrogate for inertial power (Fomunung et al., 1999). We used va^2 to remove the distinction between negative and positive values. The raw measured fuel consumption had a minimum measurement step size of 80 ml, and an update rate that varied between 100 ms and a number of seconds. The cumulative fuel consumption data were interpolated to 100 Hz with trapezoids between connecting points. To calculate the instantaneous fuel consumption in cm^3/km (used in the location-specific analysis, see Section 2.7), the difference values of the cumulative fuel consumption were divided by the vehicle speed at every sampling point.

2.6.1. Calculated driving metrics

For each longitudinal and lateral signal, the following driving metrics were calculated per lap: mean, standard deviation, maximum, minimum, 10th, 25th, 50th, 75th, 90th percentiles (10 signals x 9 metrics = 90 in total). From the 90 metrics, 7 were removed because of a lack of variation (e.g., the minimum brake pressure). Twenty-five additional metrics were calculated from the longitudinal and lateral signals (see Table 3). Accordingly, a total 108 metrics of driving behaviour (90 – 7 + 25 = 108) were obtained, which were thought to be predictive of fuel consumption (based on Ericsson, 2001; Fomunung et al., 1999; Lois et al., 2019). From the fuel consumption signal, the mean fuel consumption per km (cm^3/km), and the mean fuel consumption per second (cm^3/s) were calculated (2 metrics). Appendix 2 provides the full list of all 110 metrics.

Table 3. The used signals (left column) and the 25 additional driving metrics calculated from these signals (right).

Signal	**Additional driving metrics** In addition to the listed metrics below, for each longitudinal and lateral signal, the following metrics were calculated: mean, standard deviation, maximum, minimum, and 10th, 25th, 50th, 75th, 90th percentiles (see Appendix 2 for the all 110 metrics).
Longitudinal signals	
Speed (km/hr)	-
Longitudinal acceleration (m/s^2)	The 10^{th}, 25th, 50th, 75th, 90th percentiles of the absolute values of the signal
	Number of times the absolute acceleration > 1.5 m/s^2
	Relative positive acceleration (m^2/s^3; RPA). The RPA correlates with fuel consumption (Ericsson, 2001), and is calculated as $\frac{1}{x}\int va^{+}dt$, where x = total distance, v = speed, a^{+} = positive accelerations count, negative ones are ignored.
Throttle position (%)	The percentage where no throttle was used
Brake pressure (bar)	The number of brake presses (#)
Engine RPM (RPM)	-
Eco-score (%)	Number of times eco-score below 50 (#)
(Velocity*longitudinal acceleration)^2 (va^2; m^2/s^3)	-
Lateral signals	
Lateral acceleration (m/s^2)	The 10th, 25th, 50th, 75th, 90th percentiles of the absolute values of the signal
Steering wheel angle (SWA; deg)	The 10th, 25th, 50th, 75th, 90th percentiles of the absolute values of the signal
	Steering reversal rate (SRR). The steering reversal rate was defined as the number of times that the steering wheel was reversed (McLean and Hoffmann, 1975). It was calculated by determining the local minima and maxima of the steering wheel angle, and if the difference between two adjacent peaks was greater than 2 deg, it was counted as a reversal.
Steering wheel angle speed (deg/s)	The 25th, 50th, 75th, 90th percentiles of the absolute values of the signal

2.6.2. Principal component analysis

We performed a principal component analysis (PCA) on a matrix of 110 metrics x 4617 laps (all laps combined, see Table 2). A PCA extracts the major sources of variance in terms of component scores and loadings. The first principal component in our 110-dimensional dataset contains the direction with the largest variation, and the 110th component the smallest. The correlation between variables and factors is described by the component loadings, where 0 means no correlation and 1 means a perfect correlation with the principal component. Before conducting the PCA, all metrics were rank-transformed to create a uniform distribution. Oblique rotation of the loadings was performed to improve the interpretability of the components (Fabrigar et al., 1999).

2.6.3. Cohen's d effect size to describe the effect of eco-driving, route type, and vehicle type

The impact of eco-driving, route type, and vehicle type for each driving metric was calculated using the average Cohen's $\bar{d}$ effect size, according to Eqs. 1–4.

Effect of eco-driving instructions

$$\bar{d}^{normal-ECO} = \frac{d^{normal-ECO}_{Mégane,highway} + d^{normal-ECO}_{Mégane,mountain} + d^{normal-ECO}_{Clio,highway} + d^{normal-ECO}_{Clio,mountain}}{4} \quad (1)$$

with $$d_{normal-ECO} = \frac{\mu_{normal} - \mu_{ECO}}{s},\ s = \sqrt{\frac{(s^2_{normal} + s^2_{ECO})}{2}} \quad (2)$$

where *s* is the pooled standard deviation of the score on the metric for the two compared conditions.

Effect of route type

$$\bar{d}^{highway-mountain} = \frac{d^{highway-mountain}_{normal,Mégane} + d^{highway-mountain}_{normal,Clio} + d^{highway-mountain}_{ECO,Mégane} + d^{highway-mountain}_{ECO,Clio}}{4} \quad (3)$$

$$\bar{d}^{Mégane-Clio} = \frac{d^{Mégane-Clio}_{normal,highway} + d^{Mégane-Clio}_{normal,moutain} + d^{Mégane-Clio}_{ECO,highway} + d^{Mégane-Clio}_{ECO,mountain}}{4} \quad (4)$$

2.7. Part 2: Location-specific analysis

The location-specific analysis correlated the total fuel consumption of drivers with their driving behaviour for every 5 meters of the route along the track. The road location was computed using a combination of the GPS start location (Figure 1) and a distance meter that used wheel speed as input signal.

2.7.1. Spearman's leave-one-out correlation

The Spearman's leave-one-out correlation was calculated for all laps where drivers drove the same route at least twice in a given vehicle type and eco-driving condition. The correlation coefficient was calculated between (1) driving speed (km/hr), throttle position (%), or the current fuel consumption (cm^3/km) for each 5-m segment, and (2) the average fuel consumption over all the driver's laps in the same vehicle type and eco-driving condition, except for the lap used to calculate the value in (1). Speed and throttle position were selected because, in many studies, they are considered related to fuel consumption (e.g., Ma et al. 2015), whereas the current fuel consumption is the signal from which the total fuel consumption was constructed.

The location-specific correlation coefficient was computed for the highway route and mountain route separately. The computation of the location-specific correlation coefficient for the speed signal for the highway route can be illustrated as follows. Suppose a driver drove 30 laps on the highway with the Mégane in the eco-driving condition. One lap was used to record the speed every 5 meters, and the other 29 laps were used to calculate the driver's fuel consumption in cm^3/km. This procedure was repeated 30 times for this participant, with the next lap removed and the remaining 29 laps used to calculate average fuel consumption. Together this resulted in 30 data points of the mean speed every 5 m and the overall fuel consumption for this driver. This procedure was performed for all drivers and all four combinations of route type and eco-driving instructions (1. Mégane & eco, 2. Mégane & normal, 3. Clio & eco-driving, 4. Clio & normal), provided the driver had driven at least twice in that condition (i.e., 4 drivers were removed, see Appendix A). Accordingly, a total of 2697 data points were collected for every 5 m of the highway route. In turn, for every 5 m of the highway route, Spearman's rank-order correlation between speed and fuel consumption ($n = 2697$) was computed. A strong positive correlation would mean that drivers with a higher speed at that particular location had a higher overall fuel consumption.

The same procedure was followed for the throttle position and current fuel consumption as predictor signals. Also, the same procedure was used for computing the location-specific correlations for the mountain route (1915 data points from a total of 64 drivers).

3. Results

Figure 2 shows the mean fuel consumption, mean eco-score, and mean speed per eco-driving instruction, route type, and vehicle type. The mean eco-scores confirm that all drivers have fulfilled the task of having an average eco-score of at least 90% when driving in the eco-driving condition.

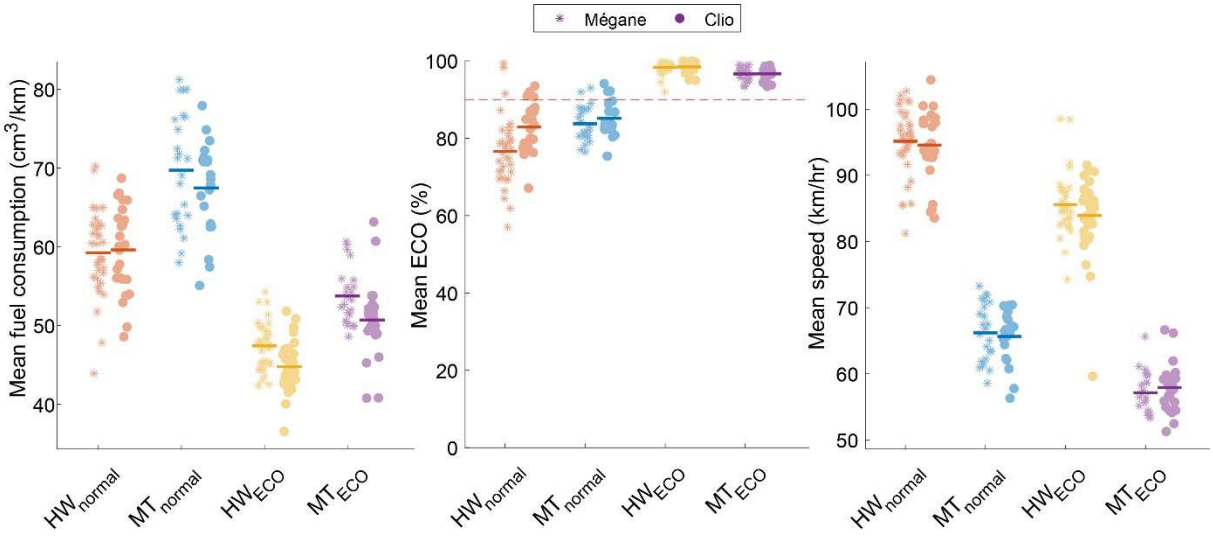


Figure 2. Mean fuel consumption per km (left), eco-score (middle), and driving speed (right) as a function of driving task, vehicle type, and route type. Each marker indicates, for one driver, the mean value averaged over all his/her driven laps.

3.1. Part 1: Predicting fuel consumption from lap-level metrics

3.1.1. Effect of eco-driving, route, and vehicle type on driving metrics

Eco-driving resulted in a lower fuel-consumption per km for both routes and both vehicles as compared to normal driving (Figure 2, left). The beneficial effect on eco-driving was greatest for eco-driving compared to normal driving ($\bar{d}$ = 3.05; this corresponds to a 23.2% fuel reduction), followed by driving on the highway route versus the mountain route ($\bar{d}$ = -1.64; 12.7% fuel reduction), and driving in the Clio instead of the Mégane ($\bar{d}$ = 0.48; 3.4% fuel reduction).

Table 4 shows the Cohen's $\bar{d}$ effect sizes for the eco-driving instructions, route type, and vehicle type, for the 50 metrics with the highest effect sizes for eco-driving instructions. Table 4 shows that both longitudinal and lateral metrics are affected by eco-driving (i.e., $\bar{d}$ > 2.0). The strongest Cohen's $\bar{d}$ values for eco-driving were found for the eco-score-related metrics, a result that can be explained by the task instructions given to participants.

Furthermore, strong effects of eco-driving were found for longitudinal acceleration-related metrics (e.g., 90th percentile of the absolute value, maximum values, and the RPA), engine-RPM-related metrics (e.g., 90th percentile, 75th percentile, and maximum values), and throttle-related metrics (e.g., 90th and 75th percentiles), mean va^2, and mean speed (see also Figure 2). As for lateral driving-related metrics, eco-driving had a large impact on the 50th percentile of absolute lateral acceleration, 50th percentile of the abs steering wheel angle (SWA), and mean SWA speed compared to normal driving. These results show that longitudinal and lateral driving metrics are highly indicative of fuel consumption.

Many of the metrics in Table 4 not only distinguish between eco-driving and normal driving, as described above, but are also sensitive to vehicle type, and especially to route type (with Cohen's $\bar{d}$ values up to 20.12, see Appendix B for more detail about the route and vehicle Cohen's $\bar{d}$ values). The strongest effects for route type were found for metrics calculated from lateral acceleration, steering wheel angle, steering wheel angle speed, and driving speed. The strongest effects for vehicle type were found for metrics calculated from the steering wheel angle, steering wheel angle speed, and the longitudinal acceleration.

3.1.2. Association between fuel consumption and driving metrics

Figure 3 shows examples of Spearman's rank-order fuel consumption correlations (which are also shown in Table 4) for three driving metrics: the eco-score, va^2, and SD throttle position. A strong association between the eco-score and fuel consumption per km can be seen (ρ = 0.73). Interestingly, SD throttle position, a fairly simple metric, had a similar correlation with fuel-consumption (ρ = 0.71) as the Renault eco-score. The strongest correlation with fuel consumption (see also Table 4) was found for the va^2 metric (ρ = 0.83).

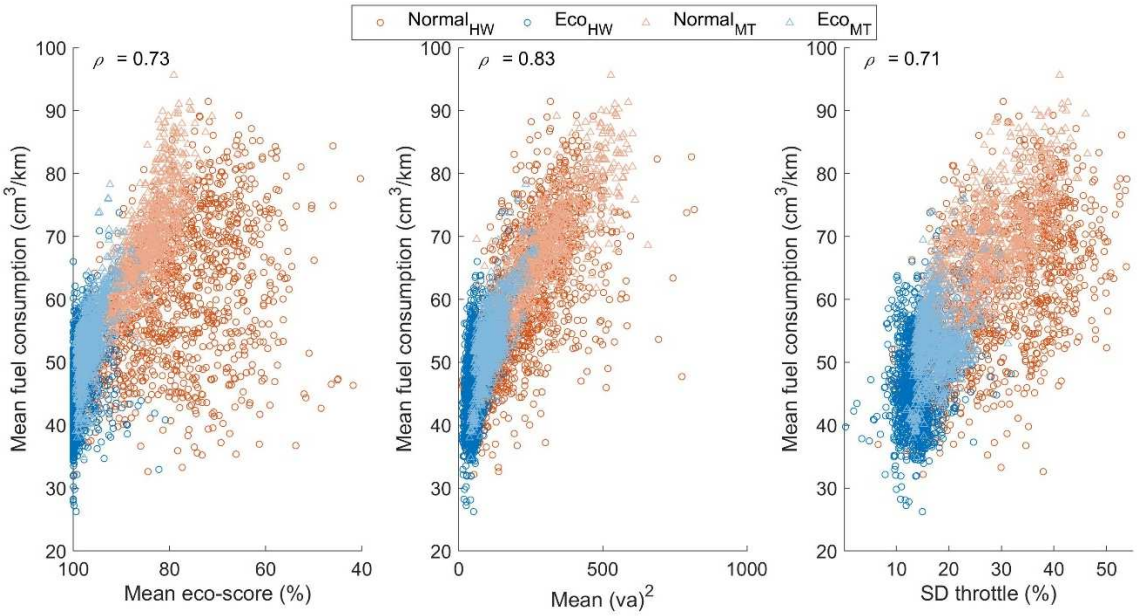


Figure 3. The Spearman's correlation (ρ) of the fuel consumption for three metrics (one marker represents one lap). No distinction is made between the Clio and Mégane.

3.1.3. Principal component analysis (PCA)

Figure 4 shows the principal component scores for all laps (n = 4617) with colour markings for the route type (left), eco-driving (middle), and vehicle type (right). The first principal component is primarily composed of (i.e., high factor loadings) metrics that yielded strong Cohen's $\bar{d}$ values for route type in Table 4 (i.e., speed, lateral accelerations, SWA, and SWA speed, see Appendix B for all factor loadings). Likewise, the second principal component is mainly composed of metrics that yielded strong Cohen's $\bar{d}$ values for eco-driving in Table 4 (i.e., eco-score, speed, fuel consumption, throttle position, engine RPM, va^2). The third principal component is composed of metrics that proved sensitive to vehicle type (i.e., SWA, va^2, longitudinal acceleration). In total, the first three principal components captured 74.9% of the total variance (1. route: 45.7%, 2. eco-driving: 21.8%, 3. vehicle type: 7.4%).

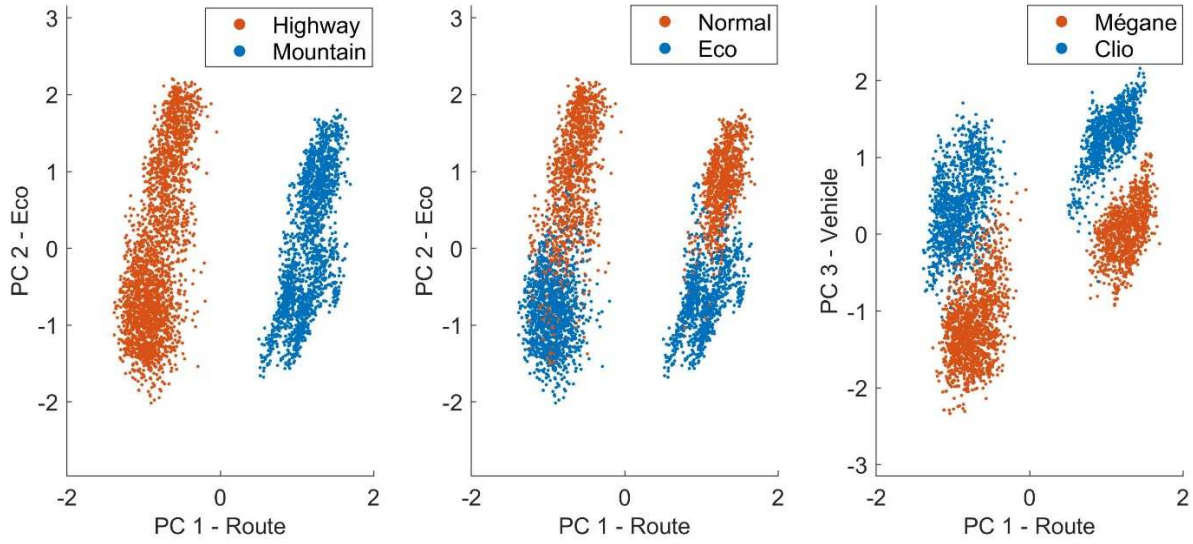


Figure 4. Scatter plot of the first two principal component scores (left and middle), and the first and third principal component scores (right) of all laps (n = 4617, one marker represents one lap). The colours indicate the route type (left), eco-driving condition (middle), and vehicle type (right).

Table 4. Fifty metrics with the highest Eco-driving Cohen's $\bar{d}$ effect sizes, and the corresponding correlation with fuel consumption for all driven laps (4617 data points).

Eco-driving Cohen's $\bar{d}$ rank & Metric		**Cohen's $\bar{d}$**			**Spearman's correlation with fuel consumption** (4617 data points)
		Eco-driving instructions (normal – eco)	**Route type** (highway – mountain)	**Vehicle type** (Mégane – Clio)	
17 Fuel consumption per km	mean	3.05	-1.64	0.48	1.00
22 Fuel consumption per s	mean	2.86	1.92	0.33	0.67
49 Principal component 1	-	2.09	-15.30	1.57	0.57
2 Principal component 2	-	3.96	-0.31	0.08	0.80
81 Principal component 3	-	1.15	-3.88	-5.13	0.39
1 Eco	SD	4.18	-0.08	0.21	0.68
3 Eco	10th perc	-3.90	-0.03	-0.20	-0.71
4 Eco	min	-3.81	1.03	0.00	-0.64
5 Eco	mean	-3.54	0.24	-0.31	-0.73
6 Engine RPM	max	3.48	-1.00	0.34	0.76
7 Eco	# times below 50	3.47	-1.78	0.30	0.74
8 Engine RPM	90th perc	3.44	-0.10	0.38	0.71
9 Engine RPM	75th perc	3.43	0.11	0.47	0.69
10 Longitudinal acceleration	90th perc of abs	3.35	-5.98	-0.29	0.72
11 Engine RPM	mean	3.22	0.65	0.51	0.64
12 va^2	90th perc	3.21	-1.78	-0.13	0.83
13 Throttle	max	3.18	-0.80	-0.64	0.68
14 Longitudinal acceleration	RPA	3.16	-3.89	-2.75	0.75
15 Longitudinal acceleration	SD	3.13	-5.22	-0.33	0.75
16 Engine RPM	SD	3.09	-1.98	0.17	0.72
18 Engine RPM	50th perc	3.04	0.64	0.50	0.62
19 Longitudinal acceleration	75th perc of abs	2.94	-5.51	-1.26	0.73
20 Eco	25th perc	-2.93	0.22	-0.39	-0.75
21 Brake pressure	mean	2.88	-3.96	-0.81	0.67
23 Long acceleration	90th perc	2.86	-4.57	-0.93	0.74
24 Brake pressure	SD	2.84	-3.69	-0.64	0.71
25 va^2	75th perc	2.78	-1.33	-0.88	0.81
26 Longitudinal acceleration	max	2.77	-5.45	-0.98	0.62
27 va^2	mean	2.77	-1.52	-0.31	0.83
28 Speed	90th perc	2.74	4.45	0.06	0.12
29 Engine RPM	25th perc	2.72	1.22	0.56	0.52
30 Brake pressure	max	2.62	-3.16	-0.39	0.69
31 Speed	75th perc	2.46	4.69	0.09	0.09
32 Longitudinal acceleration	10th perc	-2.46	5.09	0.26	-0.59
33 Throttle	SD	2.46	-0.91	-0.90	0.71
34 Speed	max	2.45	3.80	0.04	0.14
35 Lateral acceleration	50th perc of abs	2.39	-2.25	0.07	0.74
36 Throttle	90th perc	2.37	-0.03	-0.99	0.67
37 Speed	SD	2.37	-1.99	0.08	0.78
38 Longitudinal acceleration	min	-2.34	3.38	0.13	-0.71
39 Engine RPM	10th perc	2.33	1.64	0.55	0.40
40 va^2	50th perc	2.32	-0.57	-1.76	0.67
41 Eco	50th perc	-2.28	0.17	-0.42	-0.71
42 Longitudinal acceleration	50th perc of abs	2.24	-4.09	-2.41	0.64
43 Longitudinal acceleration	75th perc	2.24	-2.74	-3.11	0.64
44 Longitudinal acceleration	# of hard brakes	2.23	-4.01	-0.64	0.62
45 va^2	SD	2.21	-1.24	0.28	0.80
46 Steering wheel angle	50th perc of abs	2.16	-8.55	1.59	0.64
47 Throttle	mean	2.15	1.14	-0.83	0.58
48 Speed	mean	2.11	6.31	0.08	0.05
50 Speed	50th perc	2.05	6.27	0.11	0.04

Note. A $\bar{d}$ larger than 0 means higher values for normal than eco, highway than mountain, and Mégane than Clio.

3.2. Location-specific analysis

Figure 5 (highway) and Figure 6 (mountain) show the results of the location-specific analysis. These figures show the mean and standard deviation of recorded signals of all laps for both normal driving (highway: n = 1250, 53 drivers; mountain: n = 930, 38 drivers) and eco-driving (highway: n = 1449, 54 drivers; mountain: n = 988, 38 drivers) as a function of travelled distance for the two vehicles combined. In addition to the three selected predictor signals, we also visualised the instantaneous curvature (yaw rate/speed) to provide an insight into the sharpness of the curves, and the brake pedal position to provide a more complete picture of driving behaviour. The bottom panels of Figures 5 and 6 show the location-specific correlations between overall fuel consumption and driving speed, between overall fuel consumption and throttle position, and between overall fuel consumption and current fuel consumption, for the highway route (n = 2697, 84 drivers) and mountain route (n = 1915, 64 drivers), respectively.

The figures illustrate that, in the eco-driving condition, participants on average drove a substantially slower speed compared to normal driving, for most of the highway and mountain routes. For some sharp curves of the mountain road, the mean speeds in the two groups were equivalent. Lower and later throttle presses (positive values in the third subplot), and less braking (negative values in the third subplot) were found for eco-driving compared to normal-driving. Finally, when eco-driving a lower current fuel consumption was found compared to normal driving.

The bottom graphs of Figures 5 and 6, show that the correlation coefficient depends on the route and the location along the route. Higher peak correlations occur for driving speed (highway route: $\rho = 0.69$, mountain route: $\rho = 0.83$) than for fuel consumption (highway route: $\rho = 0.56$, mountain route: $\rho = 0.71$) and throttle position (highway route: $\rho = 0.56$, mountain route: $\rho = 0.72$). The throttle and fuel consumption exhibit a more volatile correlation with fuel consumption than the driving speed. The correlations for fuel consumption and throttle position decrease considerably, and even become negative, at the beginning of turns. Figure 7 shows a scatter plot for the maximum and minimum correlation of the mountain route (indicated with triangle and circles in Figure 6, respectively). A negative correlation for speed ($\rho = -0.13$), throttle ($\rho = -0.50$), or fuel consumption ($\rho = -0.38$) means that drivers with a higher driving speed, deeper throttle depression, and higher fuel consumption at that particular location had a lower overall fuel consumption.

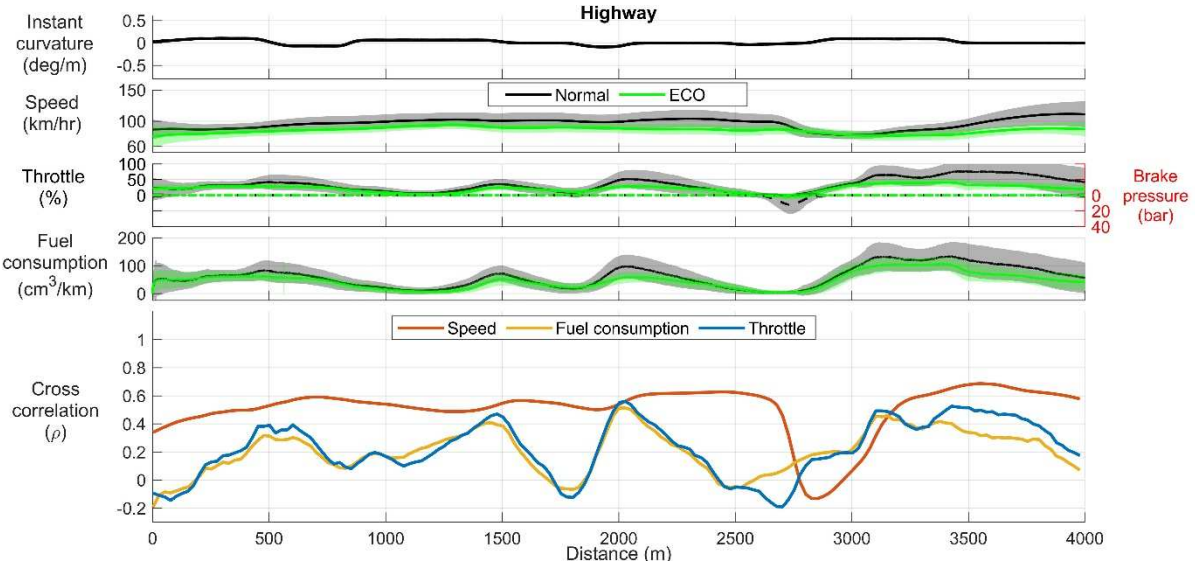


Figure 5. Location-specific results for the highway route for the normal (n = 1250, 53 drivers) and eco-driving (n = 1449, 54 drivers) conditions . The bottom figure shows the leave-one-out correlation (n = 2697, 84 drivers).

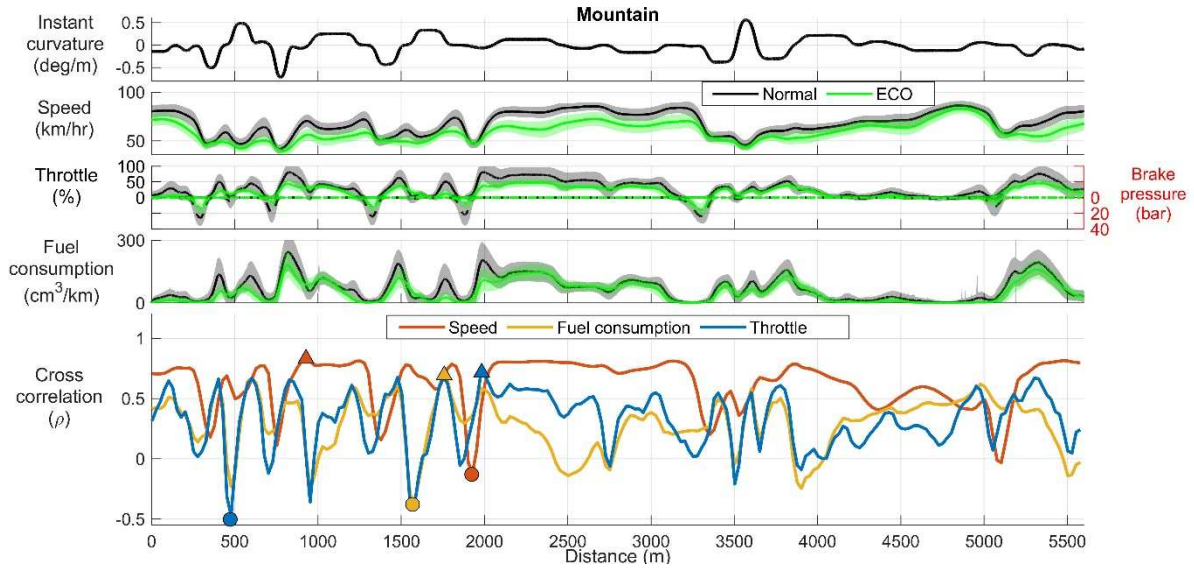


Figure 6. Location-specific results for the mountain route for the normal (n = 930, 38 drivers) and eco-driving (n = 988, 38 drivers) conditions. The bottom figure shows Spearman's leave-one-out correlation (n = 1915, 64 drivers).

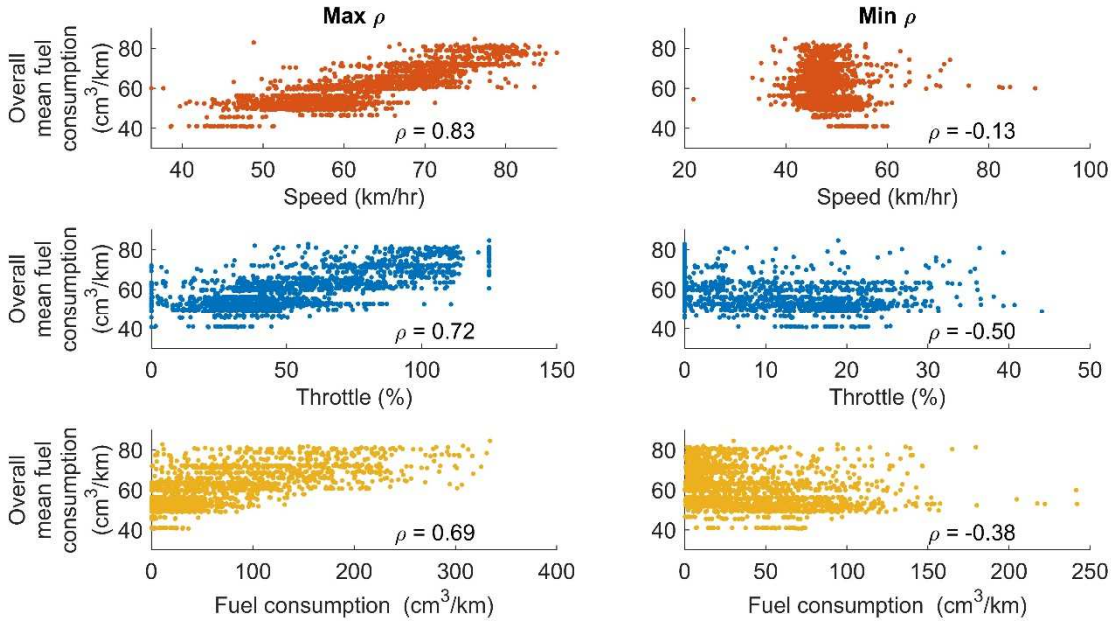


Figure 7. Scatter plots of the maximum (left) and minimum (right) Spearman's leave-one-out correlation between mean fuel consumption and three driving metrics. The triangles and circles in Figure 6 mark the location of the maximum and minimum, respectively.

4. Discussion

The purpose of this study was to predict fuel consumption from driving behaviour measurements, with the underlying motivation to allow improvements in eco-driving feedback and training applications. In the first part of the analysis, we correlated 110 driving metrics and three PCA components with fuel consumption at the level of laps on the test track. The goal of this analysis was to determine which metrics are most strongly associated with fuel use, to examine how these metrics are associated with each other, and to investigate how much these metrics are influenced by route and vehicle type. In the second part of the analysis, we examined which part of the route is predictive of fuel consumption by correlating driving behaviour at a large number of points along the route with drivers' fuel consumption for the entire route.

Part 1: Predicting fuel consumption from lap-level metrics

Compared to normal driving, eco-driving resulted in a 23.2% reduction in fuel consumption per kilometre, corresponding to a Cohen's $\bar{d}$ of 3.05 (i.e., a large difference; more than 3 times the standard deviation). Compared to the literature, such fuel reduction benefits are on the higher side (see also Alam & McNabola, 2014; Huang et al., 2018; Xu et al., 2016), which can be explained by the eco-score received on the dashboard, the extensive eco-training received for all 91 drivers, and the lack of surrounding traffic and traffic lights. In summary, the experimental methods (i.e., the eco-driving training, and test track setting) were successful in eliciting vastly different driving styles and corresponding fuel consumption levels to be analysed further.

The metrics that proved to be most sensitive to the eco-driving instructions (i.e., metrics yielding the largest eco-driving Cohen's $\bar{d}$) were metrics associated with engine RPM, longitudinal acceleration, and throttle input. Note that a high eco-driving Cohen's $\bar{d}$ for a particular metric does not imply that this metric is a practical index of eco-driving. In fact, the speed and longitudinal metrics had a high Cohen's $\bar{d}$ for *eco-driving*, but an even higher Cohen's $\bar{d}$ for *route type*, which indicates that these metrics are more influenced by the driven route than the adopted eco-driving style. We advocate that, ideally, an eco-score should correlate strongly with consumption and should be interpretable in different road environments and for different vehicles. In other words, when driving in an energy-demanding environment (e.g., mountain), drivers should not receive a notification that they drive eco-unfriendly. Of course, such information might still be valid if drivers need to be informed that they selected an eco-unfriendly route, but in practice, drivers may not be able to adjust their route. Similar statements

were made by Andrieu and Saint Pierre (2012), Shi et al. (2015) and Dib et al. (2014), who proposed to normalise fuel consumption to the road environment.

The principal component analysis results complement the findings described above, where the largest part of the variance (45.7%) in the metrics was attributable to the route type. High component loadings were found for metrics related to speed, lateral acceleration, and steering wheel angle, suggesting that especially these metrics are impacted by route type (Appendix B). The second component showed high loadings for engine RPM, va^2, throttle, speed, and eco-score metrics. It had a large correlation with fuel consumption, but a small correlation with route and vehicle type, making it interesting to be used as an eco-score in future research. Finally, for the third component (vehicle type), high loadings were obtained for the 10^{th} percentile of the absolute longitudinal acceleration, the 10^{th} percentile of va^2, and the 75^{th} percentile of the steering wheel angles. These effects may be attributable to vehicle-specific factors such as the steering wheel gain, pedal mapping, and engine type.

The first part concludes that driving metrics are highly predictive of fuel consumption but with a considerable amount of variance attributable to route and vehicle type. There is a substantial amount of literature on the effects of eco-driving behaviour, vehicle type, and route features on fuel consumption and driving metrics (Brundell-Freij & Ericsson, 2005; Wang & Boggio-Marzet, 2018; Ma et al., 2015). Compared to the literature, our experimental protocol allowed for a more controlled investigation of eco-driving behaviour (participants were allocated to an eco-driving condition), vehicle type (in the real world, sporty drivers may choose to drive a sportier vehicle), and route (in the real word, drivers can determine their own route). The large influence of route and vehicle type on fuel consumption makes most of the metrics in their current form limitedly useful for providing drivers with advice on their driving style.

Part 2: Location-specific analysis

In the second part of this paper, we correlated driving behaviour along the lap with drivers' fuel consumption for all laps driven. We demonstrated that it makes sense to develop location-specific predictors of eco-driving, as high leave-one out correlations with fuel consumption were found for specific locations of the route. The highest correlation was found for driving speed, for both the highway route ($\rho = 0.69$) and the mountain route ($\rho = 0.83$). The correlations showed strong fluctuations along the route, with negative correlations when approaching particular curves. The negative correlations mean that, for that specific location, drivers who adopted a higher

speed, throttle, or fuel consumption per km, ended up with lower fuel consumption over the entire route. Keeping momentum while approaching a curve is advantageous because, if a higher speed is maintained throughout the curve, less acceleration is needed after the curve. Our findings correspond to Ma et al. (2015), who showed that the largest fuel consumption differences between driving styles were found in the acceleration and deceleration phases.

Our findings emphasise the importance of developing location-specific fuel-consumption/driving style predictors. Currently, researchers employ artificial intelligence and large amounts of data to create increasingly accurate predictors (Martinez et al., 2017). We argue that, at one point, adding more trip-level data, or measuring for longer periods of time, will not improve the accuracy of fuel-economy predictions anymore, but including location-specific information could. Note that the Cohen's $\bar{d}$, calculated per lap, already corrects for route and vehicle type, but it is not location-specific. If fuel consumption predictions are conducted at a trip level, valuable location-specific information is lost due to the aggregation of data. This was clearly visible from the correlation between the mean speed and fuel consumption: with, on the one hand, a very weak correlation when computed per lap (i.e., combining all route, vehicle, and eco-driving instructions: $\rho = 0.05$; Table 4) and, on the other hand, the highest leave-one-out correlation (for the mountain route $\rho = 0.83$ and the highway route $\rho = 0.69$), along with a strong eco-driving Cohen's $\bar{d}$ ($d = 2.11$). The low mean speed correlation with fuel consumption when calculated per lap can be explained by a formal fallacy (also known as the Simpson's paradox; Simpson, 1951), where, in a given environment, driving faster normally increases fuel usage, while between environments, driving faster reduces fuel usage (i.e., highway driving yields better fuel economy than driving in the mountains). A location-specific eco-driving predictor would be able to resolve this fallacy. In theory, a location-specific predictor would not even need a (long) observation window, but allows for an almost immediate prediction of the driver's overall fuel consumption or driving style based on the driver's current behaviour. Extending our location-specific predictor with external information such as information about congestion (Lois et al., 2019), static traffic features (traffic signs, traffic lights, parked vehicles), and dynamic features (other road users) may lead to even more powerful predictions.

Future studies should investigate the robustness of a location-specific predictor for other types of environments, and determine general rules for the "best" location to create a location-predictor. Based on our results, we hypothesise that the acceleration and deceleration phases are particularly suitable because these are the periods

where the standard deviation of the fuel consumption is large between drivers (e.g., beginning and the end of a curve, or near traffic lights). To practically implement a real-world location-predictor in eco-feedback systems this would require a mapping of not only road type (e.g., curvature and slope), but also the location-specific driving behaviour of a variety of drivers (a "Tesla-like" approach). As an alternative to such an exhaustive mapping, a more general set of rules could be established: for example an average road curvature of 500-m has a correlation with driving metric and fuel consumption of Y1, whereas the acceleration phase at a traffic light has a correlation of Y2. The use of location-specific information with real-vehicle CAN-data would be feasible (Melman et al. 2019).

Although this test track study allowed for a controlled driving behaviour study with real vehicles, it lacks interaction with other road elements, such as other road users and traffic lights. Future studies should investigate how our results generalise to more realistic conditions. To maintain the high control that allows for the systematic analysis used in this study, we recommend that future research is conducted with surrounding vehicles traffic on a test track. It can be expected that drivers will change their eco-driving behaviour when driving in front of or behind other vehicles, such as during car following. Finally, we note that some of our effect sizes should be interpreted with caution, as correlation does not imply causation. For example, the high eco-driving Cohen's $\bar{d}$ for the metric '50th percentile of the absolute steering wheel angle' does not imply that drivers should be advised to steer less if they want to improve their fuel economy. This finding can be explained by an underlying cause known from vehicle dynamics: taking a turn at a lower driving speed requires a somewhat smaller steering wheel angle.

We conclude that driving metrics, when calculated per lap, are strongly correlated with fuel consumption in that lap. However, a large part of the variance in the driving metrics was attributable to the route type, making trip-level metrics less suitable for real-time driver feedback. We demonstrated that location-specific measurements offer powerful and near-instantaneous fuel consumption predictions for specific locations on the route. These findings may pave the way for new eco-driving applications.

Acknowledgements

The authors would like to thank the members of Renault's car data lab, and with a special thanks to Marc Blaisius, Mathilde Eyherabide, Nelson Fernandez-Pinto, Perrine Cribier-Delande, and Raphael Puget, for making this study possible.

Disclosure statement

Timo Melman is employed by Renault Inc. and does his PhD research in collaboration with the Delft University of Technology and ENSTA ParisTech.

References

Alam, M. S., & McNabola, A. (2014). A critical review and assessment of Eco-Driving policy & technology: Benefits & limitations. *Transport Policy*, *35*, 42-49.

Allison, C., & Stanton, N. (2018) Eco-driving: the role of feedback in reducing emissions from everyday driving behaviours. *Theoretical Issues in Ergonomics Science*, *20*, 85-104.

Andrieu, C., & Saint Pierre, G. (2012, June). Using statistical models to characterise eco-driving style with an aggregated indicator. In 2012 *IEEE Intelligent Vehicles Symposium* (pp. 63-68).

Ben-Chaim, M., Shmerling, E., & Kuperman, A. (2013). Analytic modeling of vehicle fuel consumption. *Energies*, *6*(1), 117-127.

Brundell-Freij, K., & Ericsson, E. (2005). Influence of street characteristics, driver category and car performance on urban driving patterns. *Transportation Research Part D: Transport and Environment*, *10*, 213-229.

Caban, J., Vrábel, J., Šarkan, B., & Ignaciuk, P. (2019). About eco-driving, genesis, challenges and benefits, application possibilities. *Transportation Research Pr*ocedia, *40*, 1281-1288.

Dib, W., Chasse, A., Moulin, P., Sciarretta, A., & Corde, G. (2014). Optimal energy management for an electric vehicle in eco-driving applications. *Control Engineering Practice*, *29*, 299-307.

Ericsson, E. (2001). Independent driving pattern factors and their influence on fuel-use and exhaust emission factors. *Transportation Research Part D: Transport and Environment*, *6*, 325-345.

Fabrigar, L. R., Wegener, D. T., MacCallum, R. C., & Strahan, E. J. (1999). Evaluating the use of exploratory factor analysis in psychological research. *Psychological Methods*, *4*, 272.

Fomunung, I., Washington, S., & Guensler, R. (1999). A statistical model for estimating oxides of nitrogen emissions from light duty motor vehicles. *Transportation Research Part D: Transport and Environment, 4*, 333-352.

Ho, S. H., Wong, Y. D., & Chang, V. W. C. (2015). What can eco-driving do for sustainable road transport? Perspectives from a city (Singapore) eco-driving programme. *Sustainable Cities and Society, 14*, 82-88.

Huang, Y., Ng, E. C., Zhou, J. L., Surawski, N. C., Chan, E. F., & Hong, G. (2018). Eco-driving technology for sustainable road transport: A review. *Renewable and Sustainable Energy Reviews, 93*, 596-609.

Lois, D., Wang, Y., Boggio-Marzet, A., & Monzon, A. (2019). Multivariate analysis of fuel consumption related to eco-driving: Interaction of driving patterns and external factors. *Transportation Research Part D: Transport and Environment, 72*, 232-242.

Ma, H., Xie, H., Huang, D., & Xiong, S. (2015). Effects of driving style on the fuel consumption of city buses under different road conditions and vehicle masses. *Transportation Research Part D: Transport and Environment*, *41*, 205-216.

Martinez, C. M., Heucke, M., Wang, F. Y., Gao, B., & Cao, D. (2017). Driving style recognition for intelligent vehicle control and advanced driver assistance: A survey. *IEEE Transactions on Intelligent Transportation Systems, 19*, 666-676.

McLean, J.R., Hoffmann, E.R., 1975. Steering reversals as a measure of driver performance and steering task difficulty,*Hum. Factors*, *17*, 248–256, http://dx. doi.org/10.1177/001872087501700304

Melman, T., de Winter, J., Mouton, X., Tapus, A., & Abbink, D. (2019). How do driving modes affect the vehicle's dynamic behaviour? Comparing Renault's Multi-Sense sport and comfort modes during on-road naturalistic driving. *Vehicle System Dynamics*, https://doi.org/10.1080/00423114.2019.1693049

Mensing, F., Bideaux, E., Trigui, R., & Tattegrain, H. (2013). Trajectory optimisation for eco-driving taking into account traffic constraints. *Transportation Research Part D: Transport and Environment, 18*, 55-61.

Saboohi, Y., & Farzaneh, H. (2009). Model for developing an eco-driving strategy of a passenger vehicle based on the least fuel consumption. *Applied Energy, 86*, 1925-1932.

Sanguinetti, A., Kurani, K., & Davies, J. (2017). The many reasons your mileage may vary: Toward a unifying typology of eco-driving behaviors. *Transportation Research Part D: Transport and Environment, 52*, 73-84.

Sanguinetti, A., Queen, E., Yee, C., & Akanesuvan, K. (2020). Average impact and important features of onboard eco-driving feedback: A meta-analysis. *Transportation Research Part F: Traffic Psychology and Behaviour, 70*, 1-14.

Sarkan, B., Semanova, S., Harantova, V., Stopka, O., Chovancova, M., & Szala, M. (2019). Vehicle fuel consumption prediction based on the data record obtained from an engine control unit. In *MATEC Web of*

Conferences (Vol. 252, p. 06009). EDP Sciences.

Shi, B., Xu, L., Hu, J., Tang, Y., Jiang, H., Meng, W., & Liu, H. (2015). Evaluating driving styles by normalising driving behavior based on personalised driver modeling. *IEEE Transactions on Systems, Man, and Cybernetics: Systems, 45,* 1502-1508.

Simpson, E. H. (1951). The interpretation of interaction in contingency tables. *Journal of the Royal Statistical Society: Series B (Methodological), 13,* 238-241.

Sivak, M., & Schoettle, B. (2012). Eco-driving: Strategic, tactical, and operational decisions of the driver that influence vehicle fuel economy. *Transport Policy, 22*, 96-99.

Vaezipour, A., Rakotonirainy, A., & Haworth, N. (2015). Reviewing in-vehicle systems to improve fuel efficiency and road safety. *Procedia Manufacturing, 3*, 3192-3199.

Wang, Y., & Boggio-Marzet, A. (2018). Evaluation of eco-driving training for fuel efficiency and emissions reduction according to road type. *Sustainability, 10*, 3891.

Xu, Y., Li, H., Liu, H., Rodgers, M. O., & Guensler, R. L. (2016). Eco-driving for transit: An effective strategy to conserve fuel and emissions. *Applied Energy, 194*, 784-797.

Zhou, M., Jin, H., & Wang, W. (2016). A review of vehicle fuel consumption models to evaluate eco-driving and eco-routing. *Transportation Research Part D: Transport and Environment, 49*, 203-218.

Appendix A – Number of laps per participant and experimental condition

Table A1. Number of laps each participant drove the highway section and mountain section for eco-driving and normal-driving and the two vehicle types

	Mégane				Clio			
	Normal		Eco		Normal		Eco	
Participant	**HW**	**MT**	**HW**	**MT**	**HW**	**MT**	**HW**	**MT**
1	0	0	0	0	0	19	0	28
2	28	0	0	0	0	0	0	0
3	0	8	0	0	0	0	0	0
4	35	15	0	0	0	0	0	0
5	0	0	17	49	0	0	16	16
6	0	0	8	3	8	0	0	0
7	16	19	0	21	0	0	0	0
8	37	0	0	0	0	0	0	0
9	5	27	0	0	0	28	0	0
10	0	0	19	0	0	0	23	0
11	0	0	5	43	0	0	38	7
12	0	0	0	0	36	10	0	0
13	0	13	0	0	0	0	0	0
14	17	15	19	0	0	0	0	0
15	0	0	19	0	0	0	0	0
16	0	0	0	0	21	0	0	0
17	0	0	33	0	0	0	0	24
18	24	10	0	0	0	0	0	0
19	0	0	8	33	0	0	0	23
20	19	13	0	0	0	0	0	0
21	0	0	0	24	0	0	17	0
22	0	0	0	0	0	0	14	0
23	0	0	0	0	20	62	0	0
24	0	0	0	0	29	0	0	0
25	0	18	0	0	21	0	17	8
26	0	0	0	0	20	0	13	0
27	0	0	0	0	43	0	0	0
28	0	0	0	0	0	0	1	10
29	0	0	0	0	13	45	0	0
30	0	0	49	33	20	20	26	0
31	0	0	0	0	9	0	0	0
32	9	23	0	0	0	0	0	0
33	0	0	0	0	0	0	0	23
34	7	0	0	0	0	0	14	0
35	11	0	8	3	0	0	28	0
36	0	0	17	0	0	24	0	0
37	0	0	0	0	0	34	0	0
38	34	0	10	0	0	0	22	0
39	0	0	30	56	62	7	19	40
40	3	0	0	0	0	0	0	0
41	26	0	0	0	0	0	0	0
42	1	28	0	22	0	0	23	0
43	0	0	29	50	0	0	0	0
44	41	22	0	0	0	0	0	0
45	0	0	25	14	0	0	28	5
46	0	0	0	0	0	38	0	0
47	37	0	0	0	0	0	0	0
48	11	14	15	31	0	0	0	0
49	0	0	24	0	0	20	0	0
50	11	14	8	20	19	0	0	0
51	0	0	25	0	0	0	12	37
52	0	0	0	0	0	0	5	0
53	0	0	0	0	30	0	43	0
54	0	0	0	0	3	34	0	0

55	0	0	14	0	0	0	0	0
56	0	0	0	13	0	0	13	0
57	0	0	14	15	25	1	0	0
58	0	4	0	0	26	1	0	0
59	0	0	24	0	0	0	0	0
60	0	0	0	11	0	0	6	21
61	0	0	34	0	0	0	32	7
62	0	0	0	27	0	0	3	40
63	12	24	20	0	0	20	0	0
64	11	0	0	0	0	0	0	0
65	5	3	0	0	16	0	0	0
66	0	0	0	0	11	0	0	0
67	0	0	20	0	0	0	0	3
68	31	0	0	0	22	0	15	0
69	0	0	22	0	0	0	0	0
70	0	0	0	0	33	0	18	2
71	36	38	0	0	0	0	16	9
72	20	42	0	0	0	15	0	0
73	16	7	0	0	0	0	0	0
74	0	0	0	0	0	0	34	0
75	0	0	68	0	0	0	15	16
76	73	0	28	17	0	0	0	6
77	3	0	0	0	42	0	0	0
78	0	0	0	0	0	0	23	29
79	0	22	0	0	0	0	0	0
80	0	0	32	25	0	0	0	0
81	0	0	0	0	20	31	0	0
82	20	20	0	0	0	10	0	0
83	0	0	0	0	0	0	11	19
84	3	15	0	0	14	13	0	23
85	13	0	27	10	0	0	0	5
86	29	0	29	0	0	0	17	0
87	3	35	52	15	22	18	12	32
88	0	0	0	0	0	0	25	11
89	18	0	3	1	0	0	40	8
90	0	0	14	0	0	0	0	0
91	0	0	15	0	0	31	26	0
# of different drivers	34	24	35	23	25	21	34	26
# of driving sections	665	449	784	536	585	481	665	452

Appendix B – List of all 110 driving metrics, PCA loadings and their corresponding analysis results.

Table B1. Cohen's $\bar{d}$ effect size, Spearman's correlation with fuel consumption, and the PCA loadings for all 110 driving metrics

	Driving metrics	**Cohen's $\bar{d}$**			**Spearman's correlation with fuel consumption**	**PCA loadings**		
		Eco adherence (normal – eco)	**Route type** (highway – mountain)	**Vehicle type** (Mégane – Clio)	**Between laps** (4617 points)	PCA 1 Route	PCA 2 Eco	PCA 3 Vehicle
	Principal component 1	2.09	-15.30	1.57	0.57			
	Principal component 2	3.96	-0.31	0.08	0.80			
	Principal component 3	1.15	-3.88	-5.13	0.39			
1	Fuel consumption per km mean	3.05	-1.64	0.48	1.00	0.29	0.73	0.07
2	Fuel consumption per s mean	2.86	1.92	0.33	0.67	-0.41	0.91	-0.03
3	Eco mean	-3.54	0.24	-0.31	-0.73	-0.11	-0.86	0.01
4	Eco std	4.18	-0.08	0.21	0.68	0.05	0.84	-0.01
5	Eco min	-3.81	1.03	0.00	-0.64	-0.09	-0.78	0.01
6	Eco 10^{th} perc	-3.90	-0.03	-0.20	-0.71	-0.07	-0.85	0.00
7	Eco 25^{th} perc	-2.93	0.22	-0.39	-0.75	-0.21	-0.83	0.03
8	Eco 50^{th} perc	-2.28	0.17	-0.42	-0.71	-0.17	-0.83	0.08
9	Eco 75^{th} perc	-1.14	NaN	NaN	-0.46	0.00	-0.61	0.06
10	Eco 90^{th} perc	-0.41	-0.52	NaN	-0.20	0.11	-0.38	0.09
11	Eco # bellow eco 50	3.47	-1.78	0.30	0.74	0.35	0.73	-0.03
12	Speed mean	2.11	6.31	0.08	0.05	-0.83	0.62	-0.10
13	Speed std	2.37	-1.99	0.08	0.78	0.26	0.69	0.08
14	Speed max	2.45	3.80	0.04	0.14	-0.79	0.66	-0.06
15	Speed min	1.20	8.28	-0.21	-0.17	-0.81	0.41	-0.12
16	Speed 10^{th} perc	0.92	7.40	0.02	-0.11	-0.82	0.45	-0.12
17	Speed 25^{th} perc	1.47	7.21	0.08	-0.01	-0.83	0.55	-0.11
18	Speed 50^{th} perc	2.05	6.27	0.11	0.04	-0.84	0.60	-0.10
19	Speed 75^{th} perc	2.46	4.69	0.09	0.09	-0.82	0.64	-0.09
20	Speed 90^{th} perc	2.74	4.45	0.06	0.12	-0.81	0.67	-0.09
21	Long acc mean	0.14	3.76	-4.08	0.01	-0.88	0.15	0.63
22	Long acc std	3.13	-5.22	-0.33	0.75	0.63	0.46	0.21
23	Long acc max	2.77	-5.45	-0.98	0.62	0.65	0.26	0.27
24	Long acc min	-2.34	3.38	0.13	-0.71	-0.57	-0.53	-0.08
25	Long acc 10^{th} perc	-2.46	5.09	0.26	-0.59	-0.72	-0.21	-0.21
26	Long acc 25^{th} perc	-1.43	4.62	0.38	-0.42	-0.65	-0.09	-0.26
27	Long acc 50^{th} perc	0.49	1.80	-2.61	0.04	-0.82	0.10	0.72
28	Long acc 75^{th} perc	2.24	-2.74	-3.11	0.64	-0.02	0.42	0.72
29	Long acc 90^{th} perc	2.86	-4.57	-0.93	0.74	0.52	0.45	0.30
30	Long acc 10^{th} perc of abs	0.23	-2.34	-6.04	0.15	-0.17	-0.14	1.00
31	Long acc 25^{th} perc of abs	0.90	-3.40	-3.25	0.41	0.14	0.02	0.84
32	Long acc 50^{th} perc of abs	2.24	-4.09	-2.41	0.64	0.28	0.29	0.63
33	Long acc 75^{th} perc of abs	2.94	-5.51	-1.26	0.73	0.52	0.38	0.39
34	Long acc 90^{th} perc of abs	3.35	-5.98	-0.29	0.72	0.66	0.40	0.20
35	Long acc # of hard acc/dec	2.23	-4.01	-0.64	0.62	0.77	0.24	0.16
36	Long acc RPA	3.16	-3.89	-2.75	0.75	0.20	0.47	0.60
37	Throttle mean	2.15	1.14	-0.83	0.58	-0.48	0.82	0.25
38	Throttle std	2.46	-0.91	-0.90	0.71	0.03	0.74	0.36
39	Throttle max	3.18	-0.80	-0.64	0.68	0.02	0.75	0.26
40	Throttle min	NaN	NaN	NaN	-0.02	-0.01	0.00	-0.08
41	Throttle 10^{th} perc	NaN	0.86	NaN	-0.08	-0.22	0.02	-0.15
42	Throttle 25^{th} perc	0.10	3.24	-0.18	-0.15	-0.68	0.20	-0.17
43	Throttle 50^{th} perc	1.19	1.41	-0.37	0.37	-0.60	0.61	0.17
44	Throttle 75^{th} perc	1.72	-0.17	-0.87	0.72	-0.18	0.74	0.42
45	Throttle 90^{th} perc	2.37	-0.03	-0.99	0.67	-0.20	0.79	0.40
46	Throttle % no throttle	-0.54	-1.93	-0.11	0.13	0.65	-0.24	0.20
47	Brake pressure mean	2.88	-3.96	-0.81	0.67	0.61	0.40	0.19
48	Brake pressure std	2.84	-3.69	-0.64	0.71	0.55	0.49	0.16
49	Brake pressure max	2.62	-3.16	-0.39	0.69	0.52	0.54	0.11
50	Brake pressure 90^{th} perc	0.96	-1.37	-0.76	0.37	0.31	0.14	0.28
51	Brake pressure # of brakes	1.36	-3.93	0.10	0.51	0.82	0.12	0.08
52	Engine RPM mean	3.22	0.65	0.51	0.64	-0.09	0.96	-0.15

53	Engine RPM std	3.09	-1.98	0.17	0.72	0.35	0.64	0.11
54	Engine RPM max	3.48	-1.00	0.34	0.76	0.20	0.82	0.03
55	Engine RPM min	1.28	2.17	0.04	0.10	-0.56	0.51	-0.09
56	Engine RPM 10th perc	2.33	1.64	0.55	0.40	-0.31	0.85	-0.25
57	Engine RPM 25th perc	2.72	1.22	0.56	0.52	-0.21	0.92	-0.22
58	Engine RPM 50th perc	3.04	0.64	0.50	0.62	-0.09	0.93	-0.17
59	Engine RPM 75th perc	3.43	0.11	0.47	0.69	0.02	0.93	-0.12
60	Engine RPM 90th perc	3.44	-0.10	0.38	0.71	0.06	0.91	-0.05
61	va2 mean	2.77	-1.52	-0.31	0.83	0.21	0.81	0.20
62	va2 std	2.21	-1.24	0.28	0.80	0.32	0.80	0.03
63	va2 max	1.89	-1.13	-0.16	0.73	0.30	0.73	0.09
64	va2 10th perc	0.63	-0.27	-3.68	0.16	-0.42	-0.01	1.05
65	va2 25th perc	1.33	-0.60	-2.53	0.43	-0.26	0.23	0.93
66	va2 50th perc	2.32	-0.57	-1.76	0.67	-0.15	0.59	0.65
67	va2 75th perc	2.78	-1.33	-0.88	0.81	0.09	0.75	0.38
68	va2 90th perc	3.21	-1.78	-0.13	0.83	0.27	0.79	0.16
69	Lat acc mean	0.00	12.87	-1.10	-0.23	-0.94	0.26	0.08
70	Lat acc std	1.69	-3.63	0.13	0.66	0.75	0.38	0.03
71	Lat acc max	0.85	-2.63	-0.16	0.55	0.76	0.23	0.08
72	Lat acc min	-0.94	3.64	-0.08	-0.57	-0.76	-0.27	-0.04
73	Lat acc 10th perc	-1.77	5.55	-0.42	-0.63	-0.82	-0.30	-0.01
74	Lat acc 25th perc	-1.93	8.75	-2.00	-0.53	-0.98	-0.16	0.21
75	Lat acc 50th perc	-0.33	15.02	-2.72	-0.33	-1.02	0.10	0.28
76	Lat acc 75th perc	1.66	2.46	-0.15	0.20	-0.68	0.69	-0.04
77	Lat acc 90th perc	1.59	-1.70	-0.02	0.70	0.44	0.60	0.05
78	Lat acc 10th perc of abs	1.00	-1.43	-1.96	0.27	-0.06	0.03	0.66
79	Lat acc 25th perc of abs	1.96	-3.56	-2.18	0.52	0.45	0.13	0.51
80	Lat acc 50th perc of abs	2.39	-2.25	0.07	0.74	0.46	0.65	0.03
81	Lat acc 75th perc of abs	1.77	-2.80	0.08	0.71	0.62	0.49	0.06
82	Lat acc 90th perc of abs	1.34	-3.10	0.05	0.63	0.72	0.35	0.05
83	SWA mean	1.49	14.94	1.95	-0.17	-0.67	0.42	-0.41
84	SWA std	1.45	-17.48	2.11	0.57	1.02	0.20	-0.28
85	SWA max	0.92	-15.16	2.15	0.48	1.06	0.13	-0.34
86	SWA min	-0.60	20.12	-1.57	-0.50	-0.97	-0.09	0.18
87	SWA 10th perc	-0.96	15.61	-1.04	-0.53	-0.90	-0.09	0.06
88	SWA 25th per	-0.02	15.30	-0.22	-0.33	-0.84	0.20	-0.12
89	SWA 50th perc	1.23	6.51	1.33	-0.20	-0.72	0.37	-0.28
90	SWA 75th perc	1.74	-0.25	2.20	0.42	0.36	0.65	-0.71
91	SWA 90th perc	1.75	-10.85	2.60	0.54	1.04	0.20	-0.33
92	SWA 10th perc of abs	0.96	-4.26	0.53	0.44	0.82	0.14	-0.08
93	SWA 25th perc of abs	1.73	-9.06	1.11	0.50	0.92	0.14	-0.09
94	SWA 50th perc of abs	2.16	-8.55	1.59	0.64	0.92	0.28	-0.13
95	SWA 75th perc of abs	1.86	-12.75	2.33	0.58	1.01	0.23	-0.27
96	SWA 90th perc of abs	1.31	-15.92	2.22	0.53	1.04	0.17	-0.32
97	SWA SRR	0.65	-2.11	0.61	0.41	0.75	0.17	-0.15
98	SWA speed mean	-0.11	-1.33	0.14	0.10	0.26	-0.08	0.05
99	SWA speed std	1.18	-7.80	0.99	0.54	0.95	0.17	-0.12
100	SWA speed max	0.41	-3.89	0.33	0.40	0.89	-0.02	-0.04
101	SWA speed min	-0.32	5.02	-0.45	-0.38	-0.89	0.05	0.03
102	SWA speed 10th perc	-1.31	5.80	-0.67	-0.53	-0.90	-0.16	0.03
103	SWA speed 25th perc	-0.90	3.63	7.27	-0.39	-0.54	-0.02	-0.34
104	SWA speed 50th perc	NaN	NaN	NaN	-0.01	-0.02	0.02	0.00
105	SWA speed 75th perc	0.76	-5.11	-5.71	0.35	0.59	-0.10	0.39
106	SWA speed 90th perc	1.32	-6.00	0.76	0.53	0.91	0.15	-0.06
107	SWA speed 25th perc of abs	NaN	NaN	NaN	0.15	0.13	0.01	0.24
108	SWA speed 50th perc of abs	0.79	-5.10	-14.88	0.37	0.59	-0.07	0.38
109	SWA speed 75th perc of abs	1.31	-5.69	0.89	0.53	0.96	0.16	-0.14
110	SWA speed 90th perc of abs	1.34	-7.69	0.92	0.54	0.93	0.18	-0.09